Influence of oscillation modes on the line width of rf emissions in MgO based nanopillars

G. Hrkac,[1,a)] A. Goncharov,[1] J. Dean,[1] T. Schrefl,[1,2] Joo-Von Kim,[3] T. Devolder,[3] C. Chappert,[3] S. Cornelissen,[4] W. van Roy,[4] and L. Lagae[4]
[1]*Department of Engineering Materials, University of Sheffield, Sheffield S1 3JD, United Kingdom*
[2]*St. Pölten University of Applied Science, St. Pölten A-3100, Austria*
[3]*Institut d'Electronique Fondamentale, UMR 8622, CNRS, 91405 Orsay, France and UMR 8622, Université Paris-Sud, 91405 Orsay, France*
[4]*IMEC, Kapeldreef 75, B-3001 Leuven, Belgium*

(Received 17 March 2010; accepted 25 May 2010; published online 30 July 2010)

We present a numerical study of oscillation modes in magnetic tunnel junction nanopillars and investigate the frequency and the full width at half maximum of the power spectrum as a function of applied field and applied current. We show that the line width reaches a minimum of 14.5 MHz as the system approaches the threshold current, and increases sharply to 308 MHz as the current is increased beyond the threshold current. The initial line narrowing is due to an increased coherence in the uniform precession mode, while the line broadening above threshold arises from the intrinsic oscillator nonlinearity combined with overlapping contributions from edge modes. We show that these results are in good agreement with recent experiments on MgO-based oscillators. © *2010 American Institute of Physics*. [doi:10.1063/1.3456497]

I. INTRODUCTION

It is well established that a sufficiently large spin polarized current can impose a torque on a nanoscale ferromagnet that can either reverse magnetization (switching) or excite a stable oscillation of the magnetization.[1–4] The switching and the oscillation of the magnetization of a thin ferromagnetic layer have been experimentally observed in spin vales[5–10] and magnetic tunnel junctions (MTJs).[11–14] Although the spin polarized current necessary to switch the magnetization in an MTJ is similar to that for spin valves, there is maximum value for the current that can be applied before the breakdown of the tunnel barrier occurs. Taking these considerations into account, experiments have shown that MgO tunnel barriers in CoFe/MgO/CoFe pillars give the best performance so far, characterized by a high tunnel magnetoresistance (TMR) ratio of 200 % and spin polarization ratio of nearly 60 %.[15–17]

The basic structure of a MTJ is composed of two ferromagnetic layers (CoFe), which are separated by a thin insulator (MgO). The magnetization of one of the ferromagnetic layers is fixed compared to the other. This is achieved by either an increased layer thickness compared to the second ferromagnetic layer or by exchange biasing the ferromagnetic to a synthetic antiferromagnet.[16,18]

While MTJs based on MgO hold much promise for potential applications as microwave oscillators, there remain a number of open questions concerning crucial parameters like power output and line width. In one previous study,[19] it was shown that the oscillator nonlinearity leads to an intrinsically higher noise level with a weak dependence on the temperature, in contrast to usual thermal broadening where a linear or square-root dependence on temperature is expected.[20]

In this paper we show that another important mechanism for line-broadening in MTJs involves the overlap of different excitation modes (edges modes), which is brought to light by studying the different magnetic modes excited by the spin torque. We show that once the applied current approaches the threshold current the magnetic modes become more uniform and uniform rotational precession can be observed. By increasing the current further, the magnetization behavior becomes more nonuniform and the peak disperses and the signal can't be distinguished from the background noise anymore. To quantify these effects we study the line width as function of current and the rf frequency as function of current and applied field. In the first step we study rf emissions in MgO based nanopillars fabricated by Singulus and measured by the Tunamos consortium.[21] The aim is to verify and reproduce the frequencies of the measured rf emission for different currents and field strengths. In the second step we make a detail analysis of the magnetization in time to understand the nature of emissions in MTJs and to explain the line width behavior as function of threshold current. We show that the oscillator nonlinearity on the line broadening and the intrinsic noise originates from an overlap of different oscillation modes and not temperature.

II. THEORY

In our micromagnetic model we start from the total Gibbs free energy, which is obtained using a hybrid finite element/boundary element method. We numerically solve the quasi static Maxwell equations and the Landau–Lifshitz–Gilbert equation (LLG), by taking into account the nonuniformity of the magnetization, and consequently the spatial change of the resistance as proposed by Slonczewski[22] in 2005, and the local current is calculated using the Brinkman

[a)]Electronic mail: g.hrkac@shef.ac.uk.

model.[23] The LLG equations are expended with the spin torque term derived by Slonczewski from circuit theory

$$(1+\alpha^2)\frac{d\mathbf{m}}{d\tau} = -\mathbf{m}\times\mathbf{h}_{\text{eff}} + \frac{1}{M_s}\alpha\mathbf{m}\times(\mathbf{m}\times\mathbf{h}_{\text{eff}}) - \mathbf{N}, \tag{1}$$

with the spin transfer torque N describing the effects caused by the spin-polarized current. The magnetization vector $m = M/M_s$ is the magnetization M normalized by the saturation magnetization M_s, α is the Gilbert damping constant, τ the time measured in units of $(\mu_0|\gamma|M_s)^{-1}$ (γ is the gyromagnetic ratio), and $h_{\text{eff}}=H_{\text{eff}}/M_s$ is the normalized effective field.

The spin transfer torque N can be written in the form

$$\mathbf{N} = \frac{J_e}{J_p} g_T \mathbf{m}\times(\mathbf{m}\times\mathbf{p}). \tag{2}$$

Here J_e is the electron current density, $J_p=(\mu_0 e d M_s^2/\hbar)$ the characteristic current density of the system ($\hbar$ is the Planck constant, e the electron charge, d the free layer thickness), and p is the unit vector in the direction of the spin-polarized current. The scalar function g_T is defined as follows:

$$g_T(\theta) = 0.5\,\eta_T[1+\eta_T^2\cos(\theta)]^{-1}, \tag{3}$$

where η_T is the polarization and $\cos(\theta)=m\cdot m_P$ is the angular function of the normalized magnetization of the free layer m and the fixed layer m_P. The inhomogeneous current distribution and the Oersted field produced by the current are taken into account by solving Maxwell equations.

The local current is computed from the tunneling conductance, which is based on the phenomenological Brinkman model.[23] The local current J is defined as

$$J = G_0 V + \Delta G\cos(\theta)V, \tag{4}$$

with V representing the bias voltage. The constant part of the conductance G_0 is given as

$$G_0 = \left[1 - \frac{A_0\Delta\phi}{16\phi^{3/2}}eV + \frac{9A_0^2}{128\phi}(eV)^2\right][R_{\text{junction}}(1+\text{TMR})]^{-1} \times\left(1-\frac{\text{TMR}}{2}\right) \tag{5}$$

and ΔG the dynamical part of the conductance

$$\Delta G = \left[1 - \frac{A_0\Delta\phi}{16\phi^{3/2}}eV + \frac{9A_0^2}{128\phi}(eV)^2\right][R_{\text{junction}}(1+\text{TMR})]^{-1} \times\left(\frac{\text{TMR}}{2}\right), \tag{6}$$

with $A_0=[4l(0.8\ \text{m})^{1/2}]/3\hbar$ being a constant consisting of the barrier thickness l, the electron mass m, and the Planck constant $\hbar$. The resistance R_{junction} is in our case 250 Ω and the TMR ratio 0.4. The main advantage of the Brinkman model is that it gives the voltage as function of current, time and temperature which can be used as a direct input for complementary metal-oxide semiconductor circuits and impedance models.

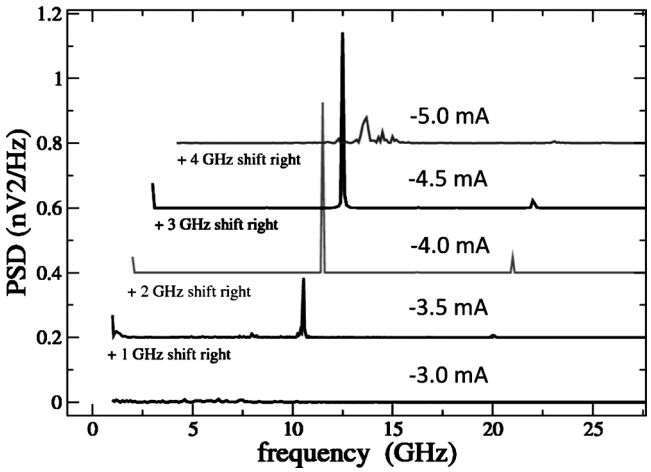

FIG. 1. Simulated PSD of voltage fluctuations for different applied currents (−3 to −5 mA). For better presentation the graphs were shifted along the x-axis for a cumulative 1 GHz and for a cumulative 0.2 along the y-axis.

III. SIMULATIONS AND RESULTS

The stack we simulated consists of 3 nm CoFeB layer (free layer)/1.4 nm MgO layer/2 nm CoFeB synthetic antiferromagnet (SAF)1 layer/0.8 nm Ru layer/2 nm CoFe SAF2/20 nm PtMn layer. The material parameters used in our system are as follows: CoFe ($A=24\times10^{-12}$ J/m, $\mu_0 M_s=2.14$ T) and CoFeB ($A=28.4\times10^{-12}$ J/m, $\mu_0 M_s=1.56$ T). The system was meshed with a tetrahedral basis function with an edge length of 2.5 nm, which is below the exchange length of our system and all simulation were performed at zero temperature.

We start from an antiparallel configuration between the free and the pinned SAF layer. Once the remanent state is calculated we perform a current sweep from −6 to 6 mA. Stable oscillations have been found in a current regime between −3 and −5 mA for an applied field of 75 mT (in plane) and between the −5 and −6 mA for an applied field of 50 mT. By going to higher applied fields the oscillations become more nonuniform with a bad signal to noise ratio.

In Fig. 1, we show the calculated voltage power spectral density (PSD) for different currents for an applied field of 75 mT. It can be seen that once a current of −5 mA is applied a peak can be found at 9.64 GHz with a full width at half maximum (FWHM) of 308 MHz. By decreasing the current to −4.5 mA the peak blue shifts to 9.75 GHz with a very narrow line width of 14 MHz, indicating that −4.5 mA is the threshold current of the system. By further decreasing the current to −4 mA, the frequency redshifts to 9.49 GHz with a slightly larger linewidth of 17.9 MHz. A further reduction in the current to −3.5 mA a frequency of 9.5 GHz can be observed with a line width of 43.6 MHz. For lower currents no rf oscillation are observed.

The same current sweep was performed for applied fields of 0, 25, 50, 100, and 125 mT. For the fields below 50 mT no rf oscillations are observed for any kind of current. For the 50 mT regime, rf oscillations can be observed only in a very narrow current regime, between −5 and −5.5 mA. For higher fields, above 75 mT rf oscillations are observed but with a bad signal to noise ratio.

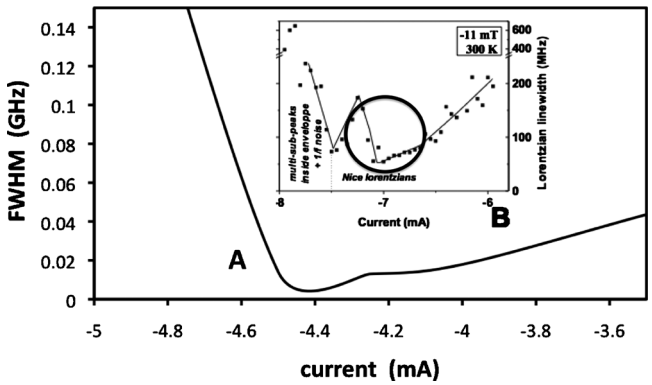

FIG. 2. (a) Full width at half maximum as function of current at zero temperature. The line width decreases with increasing current, till the threshold current at −4.5 mA is reached and increase thereafter. (b) Experimental measurement of line width vs current for a MTJ (nominal composition: 3nm CoFeB layer/1.4nm MgO/2nm CoFeB SAF1/0.8nm Ru/2nm CoFe SAF2) at 300 K.

Second we perform a Lorentzian fit on the Fourier transformed signal of the voltage (TMR) oscillations and extract the full width at half maximum. As the simulations were performed at zero temperature the FWHM analysis is a comparable study to quantify the dispersion of the signal as it approaches the threshold current and thereafter. Figure 2 gives the FWHM of the Fourier transformed signal as function of current. It can be clearly seen that the line width decreases as it approaches the threshold current, which is −4.5 mA. In the inset of Fig. 2 we show an experimental measurement of line width as a function of current for a nominal identical MTJ at 300 K. Although there is a difference in the applied current values the simulations reproduce the asymmetric trend and the finite line width as found in the experiment.

To understand the narrow line width around −4.5 mA (see Fig. 2), we studied the magnetic modes of our sample in the time domain. First we analyzed the change of the amplitude of the magnetization in plane as function of time, as shown in Fig. 3.

Simulations were performed over a time period of 100 ns. As it can be seen in Fig. 3, the amplitude for the threshold current of −4.5 mA is stable and shows only small changes in magnitude. The results for −5 mA on the other hand show

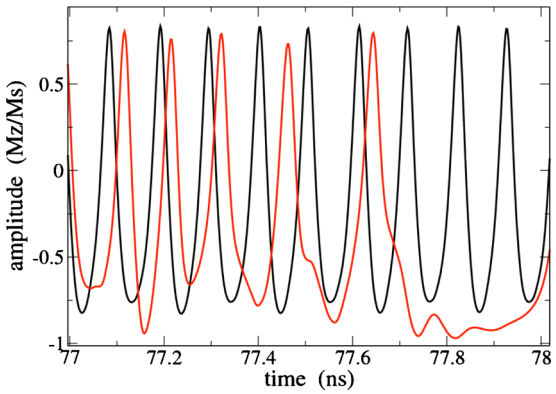

FIG. 3. (Color online) Amplitude of the magnetization in z as function of time, for an applied field of 75 mT and current of −4.5 (black) and −5.0 mA (red).

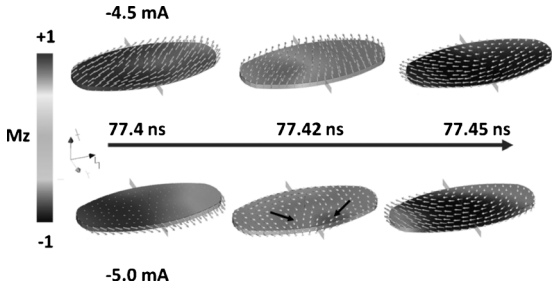

FIG. 4. Snapshot of the magnetization configuration of the free layer for −4.5 and −5 mA with an applied field of 75 mT at different times.

not only a huge change in the magnitude of the amplitude but also an overlap of different modes, as shown by the red curve in Fig. 3 around 77.5 ns and a destructive interference at 77.8 ns. In the following figures we show different magnetization states for both cases.

We compare the modes for the −4.5 and the −5.0 mA regime in Fig. 4. For better comparison we choose the magnetization states from the same time range as in Fig. 3. The magnetization snapshots show a nearly uniform rotation of the magnetization for the −4.5 mA regime throughout the whole sample. Only at the edges the magnetization vectors are slightly out of phase which contributes to the finite line width. For the −5.0 mA regime, on the other hand, the magnetization starts uniform as in the previous case but at 77.42 ns becomes less uniform. The two black arrows in Fig. 4 show the magnetization direction of the edge modes which propagate to the center of the sample and which are highly out of phase. At 77.45 ns, a C-like state of the magnetization can be observed.

It can be derived from the amplitude behavior and the analysis of the magnetization configurations that only near the threshold current a uniform rotational precession can be observed. At lower currents no oscillations behavior can be observed, and at higher currents the oscillations become more nonuniform due to edge modes which oscillate out of phase.

IV. CONCLUSIONS

We have performed a numerical study on oscillation modes in MgO MTJs and compared them with experiments. We investigated the frequency and FWHM as function of applied field and applied current. The study shows that the line width reaches a minimum as the system approaches the threshold current, and gets worse as the current is increased beyond the threshold current, which agrees well with the trend found in experiments[19] and Fig. 2. By performing our simulations at zero temperature we show that the line broadening and the intrinsic noise is due to different excited oscillation modes. The improvement of the line width is due to a more uniform precession, as the study of amplitude as function of time, and the magnetization configurations of the free layer have shown. Edge modes that oscillate out of phase contribute to the broadening of the FWHM.

ACKNOWLEDGMENTS

This work was supported by the Royal Society U.K.

[1]J. Slonczewski, J. Magn. Magn. Mater. **247**, 324 (2002).
[2]J. Slonczewski, J. Magn. Magn. Mater. **159**, L1 (1996).
[3]J. Slonczewski, J. Magn. Magn. Mater. **195**, 261 (1999).
[4]L. Berger, Phys. Rev. B **54**, 9353 (1996).
[5]J. A. Katine, F. J. Albert, R. A. Buhrman, E. B. Myers, and D. C. Ralph, Phys. Rev. Lett. **84**, 3149 (2000).
[6]J. Grollier, V. Cros, H. Jaffres, A. Hamzic, J. M. George, G. Faini, J. Ben Youssef, H. Le Gall, and A. Fert, Phys. Rev. B **67**, 174402 (2003).
[7]M. AlHajDarwish, H. Kurt, S. Urazhdin, A. Fert, R. Loloee, W. P. Pratt, Jr., and J. Bass, Phys. Rev. Lett. **93**, 157203 (2004).
[8]S. I. Kiselev, J. C. Sankey, I. N. Krivorotov, N. C. Emley, R. J. Schoelkopf, R. A. Buhrman, and D. C. Ralph, Nature (London) **425**, 380 (2003).
[9]I. Krivorotov, N. C. Emley, J. C. Sankey, S. I. Kiselev, D. C. Ralph, and R. A. Buhrman, Science **307**, 228 (2005).
[10]T. Devolder, C. Chappert, P. Crozat, A. Tulapurkar, Y. Suzuki, J. Miltat, and K. Yagami, Appl. Phys. Lett. **86**, 062505 (2005).
[11]G. D. Fuchs, N. C. Emley, I. N. Krivorotov, P. M. Braganca, E. M. Ryan, S. I. Kiselev, J. C. Sankey, D. C. Ralph, and R. A. Buhrman, Appl. Phys. Lett. **85**, 1205 (2004).
[12]J. S. Moodera and G. Mathon, J. Magn. Magn. Mater. **200**, 248 (1999).
[13]Z. Diao, D. Apalkov, M. Pakala, Y. Ding, A. Panchula, and Y. Huai, Appl. Phys. Lett. **87**, 232502 (2005).
[14]J. Vogel, W. Kuch, R. Hertel, J. Camarero, K. Fukumoto, F. Romanens, S. Pizzini, M. Bonfim, F. Petroff, A. Fontaine, and J. Kirschner, Phys. Rev. B **72**, 220402(R) (2005).
[15]G. D. Fuchs, J. A. Katine, S. I. Kiselev, D. Mauri, K. S. Wooley, D. C. Ralph, and R. A. Buhrman, Phys. Rev. Lett. **96**, 186603 (2006).
[16]S. Parkin, C. Kaiser, A. Panchula, P. M. Rice, B. Hughes, M. Samant, and S. H. Yang, Nature Mater. **3**, 862 (2004).
[17]S. Tsunegi, Y. Sakuraba, M. Oogane, K. Takanashi, and Y. Ando, Appl. Phys. Lett. **93**, 112506 (2008).
[18]A. A. Tulapurkar, Y. Suzuki, A. Fukushima, H. Kubota, H. Maehara, K. Tsunekawa, D. D. Djayaprawira, N. Watanabe, and S. Yuasa, Nature (London) **438**, 339 (2005).
[19]B. Georges, J. Grollier, V. Cros, A. Fert, A. Fukushima, H. Kubota, K. Yakushijin, S. Yuasa, and K. Ando, Phys. Rev. B **80**, 060404 (2009).
[20]V. Tiberkevich, A. N. Slavin, and J.-V. Kim, Phys. Rev. B **78**, 092401 (2008).
[21]http://www.imec.be/tunamos
[22]J. Slonczewski, Phys. Rev. B **71**, 024411 (2005).
[23]W. F. Brinkman, R. C. Dynes, and J. M. Rowell, J. Appl. Phys. **41**, 1915 (1970).